Expanding the classic moment-curvature relation by a new perspective onto its axial strain

T. Petschke[*1], H. Corres[1], J.I. Ezeberry[1], A. Pérez[1] and A. Recupero[2]

[1]*E.T.S.I. de Caminos, Canales y Puertos, UPM, Madrid, Spain*
[2]*DIC, UNIME, Messina, Italy*

Abstract. The moment-curvature relation for simple bending is a well-studied subject and the classical moment-curvature diagram is commonly found in literature. The influence of axial forces has generally been considered as compression onto symmetrically reinforced cross-sections, thus strain at the reference fiber never has been an issue. However, when dealing with integral structures, which are usually statically indeterminate in different degrees, these concepts are not sufficient. Their horizontal elements are often completely restrained, which, under imposed deformations, leads to moderate compressive or tensile axial forces. The authors propose to analyze conventional beam cross-sections with moment-curvature diagrams considering asymmetrically reinforced cross-sections under combined influence of bending and moderate axial force. In addition a new diagram is introduced that expands the common moment-curvature relation onto the strain variation at the reference fiber. A parametric study presented in this article reveals the significant influence of selected cross-section parameters.

Keywords: non-linear concrete; moment-curvature diagram; axial strain; creep; shrinkage; strain plane

1. Introduction

Integral edifices are statically indeterminate structures. If a horizontal structural element cannot expand or contract freely due to constraint, compatibility forces arise. In statically indeterminate concrete structures a compression force may develop due to cracking under instantaneous service load, since the quasi permanent moments are usually greater than the cracking moment, as shown by Pfeiffer (2004). Pfeiffer also pointed out the necessity to superimpose imposed deformations such as shrinkage, creep and temperature to the instantaneous strain in order to obtain reasonable forces for serviceability assessment. Commonly these problems are resolved at structural level, but in order to completely understand the physics and mechanics involved, it is fundamental to take a closer look at the cross-section behavior. The aim of this paper is to create a general understanding of a cross-section's strain variation under serviceability conditions and to elaborate it systematically. Historically, imposed deformations were considered in crack width prediction models as shown by Falkner (1969) for axial imposed deformations on restrained tensile members and by Rostásy *et al.* (1976) for imposed curvature and axial strain. The disadvantage of this

---

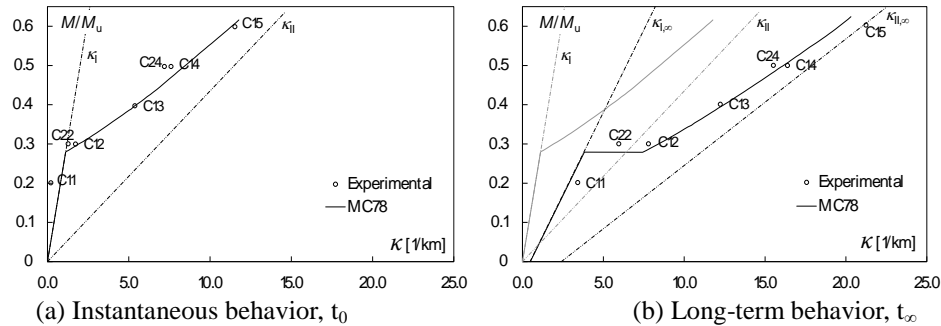∗Corresponding author, Ph.D., E-mail: tpp@he-upm.com

Fig. 1 Experimental results obtained by Jaccoud and Favre (1982) illustrating the curvature change from (a) t_0 to (b) t_∞
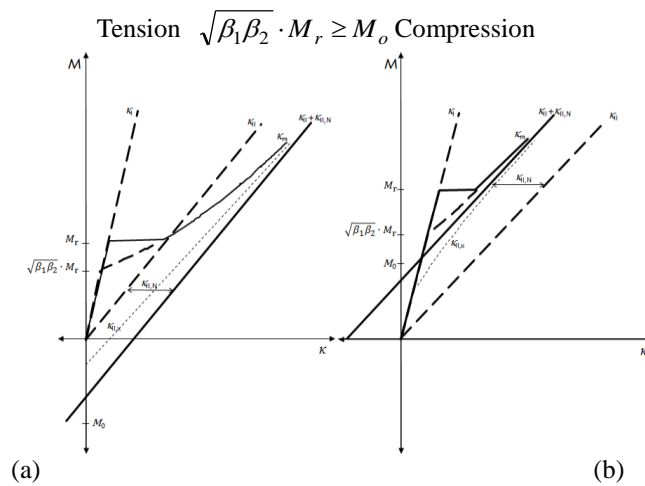

Fig. 2 The effect of (a) tension and (b) compression onto the moment-curvature relation according to Comite Europeen du Beton (CEB-FIB) (1985)

approach is its lack to consider the structural interaction. The results of many experimental studies on continuous beams have been compiled by Leonhardt (1978) to predict their deflections using the classical moment-curvature relation. The influence of creep onto the moment-curvature relation has been shown by Jaccoud and Favre (1982). With their experiments they confirmed the rotation produced in the moment-curvature relation due to an increase of curvature caused by creep under sustained loading, as shown in Fig. 1.

The effects of tension and compression axial forces onto the instantaneous moment-curvature relation, as published in Comité Europeén du Béton (CEB-FIB) (1985), are shown in Fig. 2. These basic diagrams not only provide with the simple scheme of the offset produced by axial force but also display the contribution of concrete's tensile strength and tension stiffening. More explicit research on the concrete's tensile collaboration has been contributed by Ng *et al.* (2010) and Lam *et al.* (2010).

In his thesis Camara (1988) proposed simplified diagrams to consider the effect of shrinkage
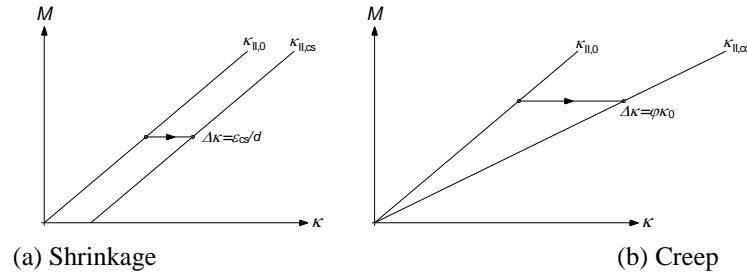
Fig. 3 The effect of (a) shrinkage and (b) creep onto the moment-curvature relation according to Camara (1988)
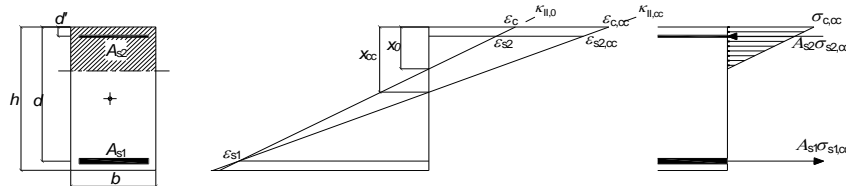

Fig. 4 Simplified creep produced strain change in a reinforced concrete cross-section according to Murcia (1991)

and creep of a reinforced concrete cross-section in cracked state onto the moment-curvature relation. While shrinkage produces a constant change of curvature, creep is linearly load-dependent and hence its effect results in a proportional increase of the curvature, as shown in Fig. 3.

A simplified approximation of shrinkage and creep consideration to evaluate long-term deflections was proposed by Murcia (1991). Wherein, he considered the effect of both actions onto the strain plane at cross-section level. This concept allows evaluating the strain increment at the reference fiber in a simple and adequate way. In Fig. 4 the approach is illustrated for creep acting onto an asymmetrically reinforced cross-section. This has been validated by Marí *et al.* (2010) with benchmark tests using a database that contained 217 different experiments. It was Pfeiffer (2004) who proposed the use of $\varepsilon_{cs} / 2$ as a simplified strain increment at the reference fiber to take into account shrinkage in case of a cracked cross-section, assuming equally to Murcia and Marí that the strain plane pivots around the tensile steel fiber. Most researchers were focusing on the prediction of short and long-term deflections Ning *et al.* (2001), Pam *et al.* (2001), Au *et al.* (2005) and Kim (2007), whereas Pfeiffer's innovative contribution was the superposition of instantaneous axial strains and long-term axial imposed deformations. Unfortunately he concentrated on axial strains and did not correlate these to the moment-curvature relation. In their work Kaklauskas and Gribniak (2011) stated that even the instantaneous moment-curvature relations are influenced by shrinkage and proposed an approach to obtain shrinkage-free moment-curvature relations without any consideration of positive instantaneous axial strains.

The authors would like to propose a new perspective of the classic moment-curvature correlation and an extension of these diagrams, by displaying the evolution of the strain in the reference fiber, usually assumed as the center of the concrete gross cross-section, and relating it to
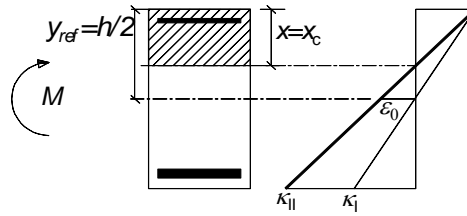
Fig. 5 Strain plane of a RC cross-section

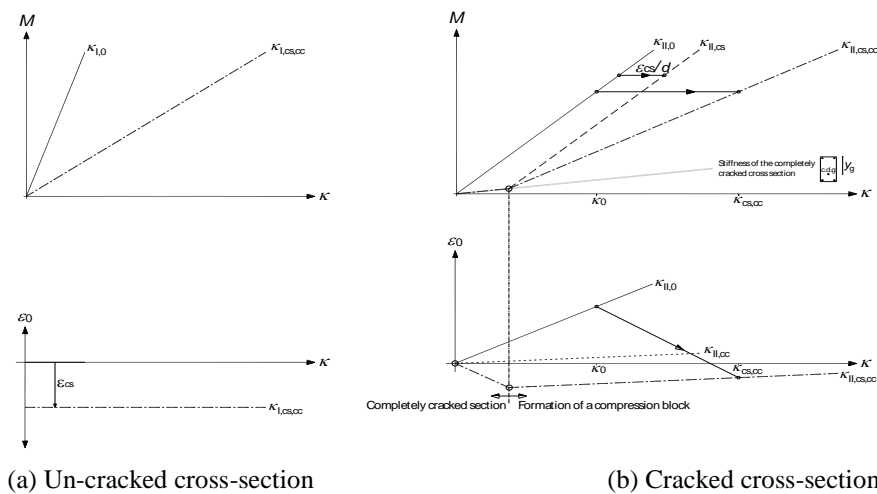(a) Un-cracked cross-section   (b) Cracked cross-section

Fig. 6 Moment-curvature-strain relation for a cross-section in un-cracked and cracked state

the cross-section's curvature. In contrast to previous studies conducted by authors like Najdanovic (1987) the focus is on integral structures' horizontal elements, which are commonly asymmetrically reinforced. These elements are designed for bending and their axial force solicitation is considered to be moderate.

2. Methodology

2.1 Strain at geometric center of the cross-section under simple bending

In order to understand this complex non-linear phenomenon, a simplified study on the theoretical behavior of concrete cross-sections under quasi-permanent serviceability conditions has been carried out. In preparation, some simplified assumptions have been agreed on, such as linear behavior of concrete in compression limiting its maximum allowable stresses to $0.6 \cdot f_{ck}$, neglecting any concrete's tensile strength. Steel is assumed to be linear. The validation of these conventions is based on ordinary serviceability analysis. Neglecting the concrete's tensile strength will provide clear display of the effects produced in moment-curvature-strain relations. The convention of signs is: negative for compressive stress and shortening strain, while positive for tensile stress and expanding strain. In Fig. 5 a cross-section is presented in un-cracked and cracked state. Neutral

fiber, x, and compression block depth, x_c, coincide. Due to the reduction of the compression block the neutral fiber rises above the center of the un-cracked cross-section, increasing the strain in the reference fiber, ε_0. Fig. 6 shows an example of an un-cracked and a cracked asymmetrically reinforced cross-section without axial force and displays the influence of the long-term effects onto the moment-curvature-strain relation. Two diagrams are displayed for each section, the moment-curvature relation and the strain-curvature relation, that way each moment relates directly to its strain by curvature. Fig. 6(a) shows, that in the un-cracked cross-section shrinkage will not have any influence onto the moment-curvature relation but will generate a constant offset at the reference fiber. The creep effect depends on the load thus creating a linear curvature increment. The strain at the reference fiber is not changed. Fig. 6(b) shows, that in cracked state this behavior changes. The most significant difference is the existence of a load dependent instantaneous strain at the reference fiber which is always positive. As shown in the scheme of Fig. 5, this is a product of cracking and the consequential adjustment of the neutral fiber. Shrinkage now not only produces a constant curvature increment in the moment-curvature correlation, but also a constant increment of the strain at the reference fiber due to the rotation of the strain plane around the tensile steel fiber according to Pfeiffer (2004). Assuming an adequate precision of the proposal made by Murcia (1991) creep also produces a rotation of the strain plane with its pivot at the tensile reinforcement fiber. Due to its load dependence it causes a linear variation in the moment-curvature and the strain-curvature relation. It should be mentioned that shrinkage acting on an asymmetrically reinforced cross-section without load influence leads, under the proposed material laws, to a completely cracked cross-section. In the moment-curvature diagram in Fig. 6(b) this is represented as a reference line.

Temperature can act in two different ways: either as a constant or as a differential temperature variation. The former will exclusively produce a constant offset in the strain-curvature diagram. The latter is usually composed by a temperature imposed curvature and a temperature imposed constant increment of strain as described before, thus acting with its differential part only onto the moment-curvature relation.

2.2 Strain at the reference fiber of a cross-section under bending and axial force

As described in literature Comité Europeén du Béton (CEB-FIB) (1985) the moment-curvature relation follows, under the presence of a compressive axial force, State I until cracking and thereafter State II. For the presence of a tensile axial force the cross-section under small bending moments is completely cracked and its stiffness is equal to that of the reinforcement considering the difference between reference fiber and c.o.g. (center of gravity) of the reinforcement. When the moment finally introduces a compression block into the cross-section the curve runs parallel to State II. As explained previously for simple bending the effects of shrinkage and creep produce an offset and a linear change onto the moment-curvature relation. Both effects reflect in the same manner in the presence of an axial compressive or tensile force, as shown in Fig. 7. The instantaneous strain, under compressive axial force and bending, increases steadily after cracking and eventually changes from negative to positive sign. Creep and shrinkage introduce a negative linear and negative constant strain increment, respectively. Under tensile axial force and bending a similar behavior can be observed originating from a positive instantaneous strain at the reference fiber.

(a) Bending and axial compressive force   (b) Bending and axial tensile force
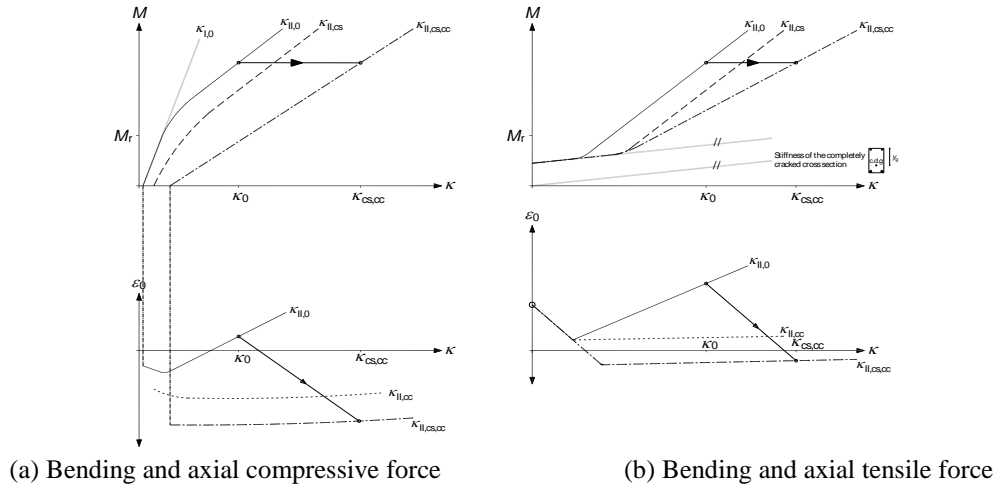
Fig. 7 Moment-curvature-strain relation for an asymmetrically reinforced cross-section under bending and axial force: (a) compressive axial force and (b) tensile axial force

2.3 Influence of concrete's tensile strength

The influence of the concrete's tensile strength will be explained by the example of the asymmetrically reinforced cross-section under instantaneous and long-term simple bending, as shown in Fig. 8. The tensile strength is considered during the analysis as an alteration of the steel stress-strain constitutive law, according to Comite Europeen du Beton (CEB-FIB) (1990). Initially the instantaneous moment-curvature relation follows the State I reference line, $\kappa_{I,0}$, due to the influence of the concrete's tensile strength. After cracking it tends towards the State II reference line, $\kappa_{II,0}$, eventually running parallel to it with a constant offset described by tension stiffening. The long-term influence reduces slightly the tension stiffening effect. The instantaneous strain-curvature relation illustrates that positive strains begin to develop under the consideration of tensile strength when the cross-section starts to crack. Beforehand, small negative strains exist. They depend on the amount of reinforcement asymmetry, which defines the difference between the reference fiber at $h/2$ and neutral fiber at the ideal cross-section's c.o.g. The long-term effects increase the negative strain of the un-cracked cross-section significantly but also reveal a development of paramount importance: the asymptotic tendency of the long-term strain, considering the concrete's tensile strength, towards the long-term strain obtained without the consideration of the concrete's tensile strength. Again, the offset is caused by tension stiffening.

This shows the important influence of the concrete's tensile collaboration, but also its involvement. In order to make the studied cross-section behavior perfectly intelligible, the authors chose to neglect the concrete´s tensile collaboration.

3. Parametric study

Based on the equilibrium and compatibility equations that can be found in the appendix, a routine was programmed. This algorithm written in MATLAB MathWorks (2002) considers the
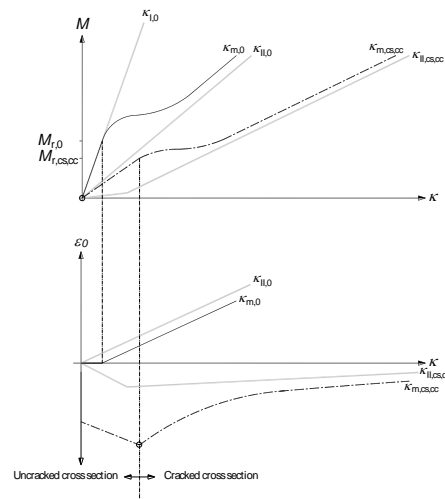
Fig. 8 Moment-curvature-strain relation for a cross-section under the consideration of concrete's tensile strength

Table 1 Cross-section values as used in the parametric study

	b [m]	h [m]	d [m]	d' [m]	ρ	ρ'
s1	0.60	0.60	0.55	0.05	0.0138	0.0009
s2	0.60	0.60	0.55	0.05	0.0138	0.0028
s3	0.60	0.60	0.55	0.05	0.0138	0.0081
s4	0.60	0.60	0.55	0.05	0.0068	0.0009
s5	0.60	0.60	0.55	0.05	0.0138	0.0009
s6	0.60	0.60	0.55	0.05	0.0244	0.0009
s7	0.40	0.90	0.85	0.05	0.0082	0.0009
s8	0.60	0.60	0.55	0.05	0.0138	0.0009
s9	0.85	0.45	0.40	0.05	0.0218	0.0009

reference fiber at the concrete gross cross-section's c.o.g. as described above. The tool allows studying the influence of different cross-section parameters.

The authors chose to center their investigation onto the following parameters: The quantity of compressive reinforcement, the quantity of tensile reinforcement, the cross-section depth and the influence of different moderate axial forces in compression or tension. Therefore three symmetrically reinforced rectangular beam cross-sections with equal gross cross-section area and equal ultimate moment were proposed.

In order to maintain clear visibility of the effects the concrete's tensile strength has been omitted in this study as explained previously. The material laws and the limitations of the represented data in the graphs are as stated above.

The concrete considered for this study has a characteristic compressive strength of $f_{ck} = 40$ MPa and a Young's modulus of $E_c = 36$ GPa. The steel's Young's modulus is $E_s = 200$ GPa. The shrinkage applied is $\varepsilon_{cs} = -329 \cdot 10^{-6}$ and the creep coefficient is $\varphi = 2.5$. In Table 1 the characteristics of the cross-sections used during the parametric study are given. The variables modified throughout the study are marked in black.
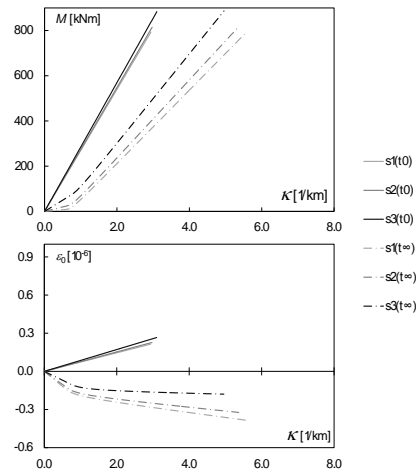
Fig. 9 Influence of the compressive reinforcement quantity

3.1 Compressive reinforcement influence

The first parameter changed was the quantity of the compressive reinforcement as shown in Table 1 sections [*s*1; *s*2; *s*3]. The results are displayed according to the moment-curvature-strain relation proposed in this article. As can be seen in Fig. 9 the influence of the compressive reinforcement quantity onto the instantaneous moment-curvature-strain relation is minimal. For the long-term correlations it can be observed that the larger amount of compressive reinforcement steel quantity has a greater restraining effect onto creep deformations, as investigated by Mayer (1962), thus leading to a smaller linear curvature increment in the moment-curvature diagram and a smaller linear strain increment in the strain-curvature diagram.

3.2 Tensile reinforcement influence

The second parameter changed was the tensile reinforcement quantity as shown in Table 1 sections [*s*4; *s*5; *s*6]. As can be seen in Fig 10. The influence of the tensile reinforcement quantity onto the moment-curvature-strain relation is important both for instantaneous and long-term loading. It can be observed that the larger amount of tensile steel quantity leads to less curvature, propagated by smaller strains in the tensile reinforcement and smaller strains in the extreme concrete compressive fiber. As a result, this is affecting the long-term behavior, since smaller stresses due to a larger compression block with smaller maximum strains lead to less creep effects. Again, the effect is exclusively visible for creep according to Mayer (1962).

3.3 Cross-section depth influence

The third parameter changed was the cross-section depth as shown in Table 1 sections
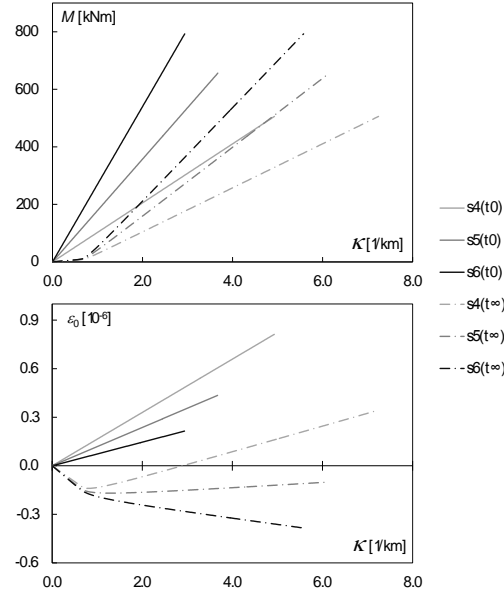
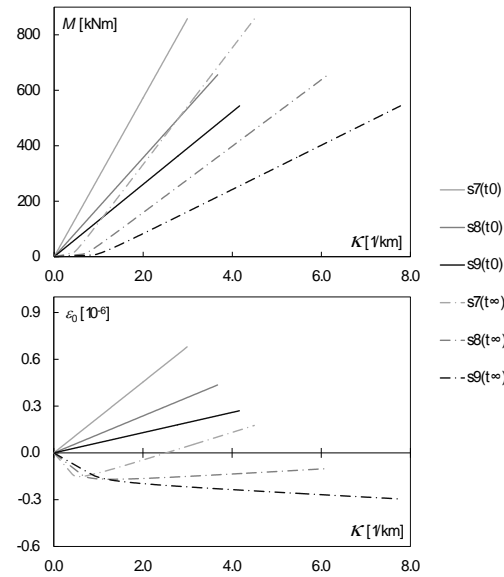Fig. 10 Influence of the tensile reinforcement quantity

Fig. 11 Influence of the cross-section depth

[*s*7; *s*8; *s*9]. Along with the cross-section depth the width and the tensile steel quantity were changed in order to provide with similar cross-section areas and an equal ultimate moment. As can be seen in Fig. 11 the influence of the cross-section depth onto the moment-curvature-strain relation is important both for instantaneous and long-term loading. A smaller effective depth leads to higher strains *ergo* stresses and hence to a greater curvature.
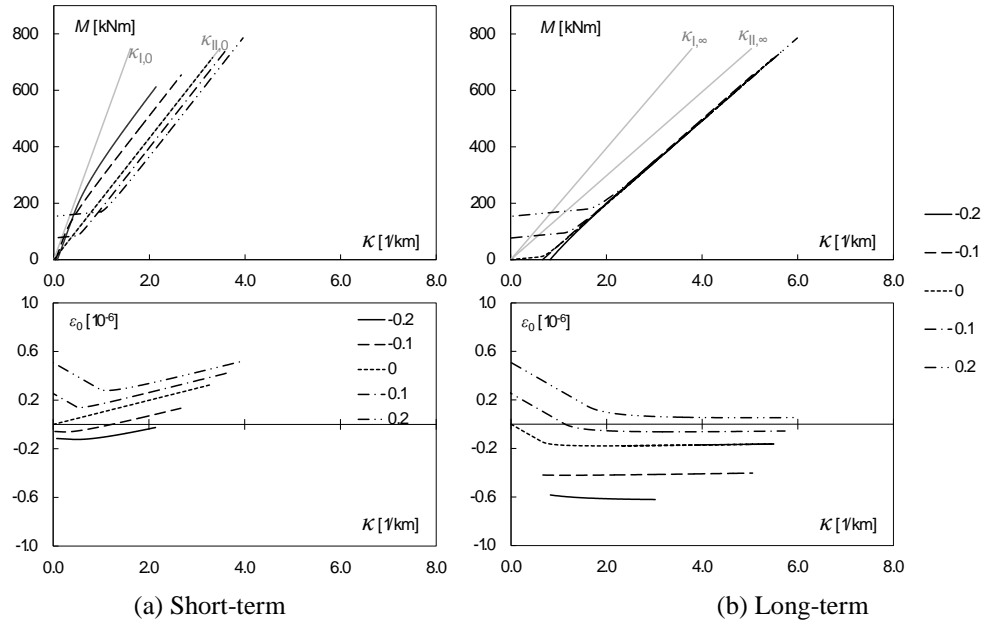
(a) Short-term   (b) Long-term

Fig. 12 Influence of moderate axial forces

3.4 Moderate axial force influence

The fourth parameter included in this study was the action of a constant, instantaneous and moderate axial force, applied as compression or tension at the reference fiber of cross-section $s1$, as shown in Table 1. The axial force was applied prior to the moment which was then increased. For this analysis a new concept of reduced axial force is proposed: if in compression, the axial force is divided by the cross-section's maximum compressive resistance $(N_{Rc} = b \cdot h \cdot f_{cd})$ accordingly $(v_c = N/N_{Rc})$. If in tension, the axial force is divided by the cross-section's maximum tensile resistance $(N_{Rt} = A_{s,tot} \cdot f_{yd})$ accordingly $(v_t = N/N_{Rt})$. The proposed range of axial force is $v = [-0.2; -0.1; 0; 0.1; 0.2]$.

Under instantaneous load there is a substantial influence of the axial forces onto the moment curvature relation, already described in Comite Europeen du Beton (CEB-FIB) (1985). The instantaneous strain receives a strain increment due to the axial force action, as shown in Fig. 12.

The long-term behavior shows a remarkable effect: all the moment-curvature relations for different axial forces tend towards the behavior of simple bending, thus revealing an equal long-term bending stiffness in all these cases within the study's boundaries. The long-term strains at the reference fiber receive constant increments through the axial forces and remain parallel.

4. Conclusions

During their research on integral structures and their statically indeterminate response the authors discovered the importance of strain and stiffness which determines the magnitude of

internal forces in such structural elements. This article is dedicated exclusively to the explanation of the concept of axial imposed deformations.

The authors discovered that the classic moment-curvature diagrams provide with insufficient information to analyze the problem at cross-sectional level.

The long-term effects, shrinkage and creep, are implicitly contained in the moment-curvature relation as shown by Camara (1988) and can be superimposed as a constant and a linear effect.

The important aspect of the strain alteration at the reference fiber cannot be derived easily from the moment-curvature correlation, therefore a new complementary diagram is proposed to provide with a complete understanding of the effects. This diagram is linked by curvature on the abscissa to the classic moment-curvature diagram and it depicts the relevant strain on the ordinate.

The basic equations of equilibrium and compatibility were used to program a routine in MATLAB MathWorks (2002) and a parametric study was carried out to examine the influence of compressive reinforcement quantity, tensile reinforcement quantity, cross-section depth and moderate axial force action onto asymmetrically reinforced concrete cross-sections. The parametric analysis shows that the least influential parameter, in the focus of this study, is the compressive reinforcement quantity.

As a follow-up an in depth analysis of cross-section and structural stiffness will be conducted to complete the analysis of imposed deformation on integral structures.

References

Au, F.T.K., Bai, B.Z.Z. and Kwan, A.K.H. (2005), "Complete moment-curvature relationship of reinforced normal- and high-strength concrete beams experiencing complex load history", *Comput. Concrete*, **2**(4), 309-324.

Camara, J. (1988), *Comportamento em serviço de estructuras de betao armado e pré-esforçado*, UTL, Lisboa, PT.

Comité Europeén du Béton (CEB-FIB) (1985), *Design manual on cracking and deformations*, EPFL, Lausanne, CH.

Comité Europeén du Béton (CEB-FIB) (1990), *Model code 1990*.

Eurocode -2 (2004), *Design of concrete structures - Part 1-1: General rules and rules for buildings*, CEN, Brussels, B.

Falkner, H. (1969), "Zur Frage der Rissbildung durch Eigen- und Zwangspannung infolge Temperatur in Stahlbetonbauwerken", Deutscher Ausschuss für Stahlbeton (Heft 208).

Jaccoud, J.P. and Favre, R. (1982), *Flèche des structures en béton armé*, Institut de Statique et Structures Béton Armé et Précontraint, EPFL, Lausanne, CH.

Kaklauskas, G. and Gribniak, V. (2011), "Eliminating shrinkage effect from moment curvature and tension-stiffening relationships of reinforced concrete members", *J. Struct. Eng.*, **137**(12), 1460-1469.

Kim, S.P. (2007), "Nonlinear analysis of RC beams based on simplified moment-curvature relation considering fixed-end rotation", *Comput. Concrete*, **4**(6), 457-475.

Lam, J., Ng, P. and Kwan, A. (2010), "Tension stiffening in concrete beams. Part 2: member analysis", *Proceedings of the Institution of Civil Engineers. Structures and buildings*, **163**(1), 29-39.

Leonhardt, F. (1978), *Vorlesung über Massivbau*, Springer, Berlin, D.

Marí, A., Bairán, J. and Duarte, N. (2010), "Long-term deflections in cracked reinforced concrete flexural members", *Eng. Struct.*, **32**(3), 829-842.

MathWorks (2002), "MATLAB program manual".

Mayer, H. (1962), "Schubversuche an Stahlbeton-Rechteckbalken mit gleichmässig verteilter Belastung", (Heft 145).

Murcia, J. (1991), "Análisis aproximado en el tiempo de secciones de hormigon en servicio. Propuesta de un nuevo factor de cálculo de flechas diferidas", *Hormigón y Acero*, (181), 9-17.

Najdanovic, D. (1987), *Contribution à la vérification de l'etat d'utilisation des colonnes sous déformations imposées*, EPFL, Lausanne, CH.

Ng, P., Lam, J. and Kwan, A. (2010), "Tension stiffening in concrete beams. Part I: FE analysis", *Proceedings of the Institution of Civil Engineers. Structures and buildings*, **163**(1), 19-28.

Ning, F., Mickleborough, N.C. and Chan, C.M. (2001), "Service load response prediction of reinforced concrete flexural members", *Struct. Eng. Mech.*, **12**(1), 1-16.

Pam, H.J., Kwan, A.K.H. and Ho, J.C.M. (2001), "Post-peak behavior and flexural ductility of doubly reinforced normal- and high-strength concrete beams", *Comput. Concrete*, (In press).

Peréz, A. (1996), *Comportamiento en servicio del hormigón estructural estudio teórico y experimental*, UPM, Madrid, ES.

Pfeiffer, U. (2004), *Die nichtlineare Berechnung ebener Rahmen aus Stahl- oder Spannbeton mit Berücksichtigung der durch aufreissen bedingten Achsendehnung*, TUHH, Hamburg, Germany.

Rostásy, F., Koch, R. and Leonhardt, F. (1976), "Zur Mindestbewehrung für Zwang von Aussenwänden aus Stahlleichtbeton", Deutscher Ausschuss für Stahlbeton (Heft 267).

Trost, H. (1967), "Auswirkungen des Superpositionsprinzips auf Kriech- und Relaxationsprobleme bei Beton und Spannbeton", *Beton- und Stahlbetonbau*, **11**(Heft 10), 230-238.

CC

Appendix

In the following the equations used to develop the algorithm for the parametric study are described. The constitutive law for the reinforcement is as follows

$$\sigma_s = E_s \cdot (\varepsilon_s - \varepsilon_T) \tag{A.1}$$

The concrete's constitutive law needs a separate description for short and long-term behavior. Short-term

$$\sigma = E_c \cdot \varepsilon_c \quad \text{if} \quad \varepsilon_c \leq 0$$
$$\sigma = 0 \quad \text{if} \quad \varepsilon_c > 0 \tag{A.2}$$

Long-term:
Shrinkage, ε_{cs}, is considered according to Eurocode -2 (2004). For creep, ε_{cc}, also the formulae of Eurocode -2 (2004) are applied. In particular, to obtain the imposed deformation produced by creep it is necessary to resolve the following equation developed by Trost (1967) to superimpose strains

$$\varepsilon(t) = \frac{\sigma_0}{E} \cdot (1 + \varphi(t, t_0)) + \frac{\sigma(t) - \sigma_0}{E} + \frac{1}{E} \int_{t=\tau_0}^{t} \frac{\partial \sigma(\tau)}{\partial \tau} \cdot \varphi(t, \tau) \cdot d\tau \tag{A.3}$$

To solve this problem Trost (1967) introduces the concept of an age adjusted Young's modulus

$$\varepsilon(t) = \frac{\sigma_0}{E} \cdot (1 + \varphi(t, t_0)) + \frac{\sigma(t) - \sigma_0}{E_o} \cdot (1 + \chi(t, t_0) \cdot \varphi(t, t_0)) \tag{A.4}$$

Where $\chi(t, t_o)$ is assumed to be 0.8 and constant as proposed by Peréz (1996).
Therefore the sum of concrete strains can be written as follows

$$\varepsilon_c(t) = \varepsilon_c + \varepsilon_{cs} + \varepsilon_{cc} + \varepsilon_T \tag{A.5}$$

$$\varepsilon_c(t) = \frac{\sigma_0}{E_c} \cdot (1 + \varphi) + \varepsilon_{cs} + \frac{\Delta\sigma}{E_c} \cdot (1 + \chi \cdot \varphi) + \varepsilon_T \tag{A.6}$$

Consequently the stress variation can be reported as

$$\Delta\sigma = \frac{E_c}{(1 + \chi \cdot \varphi)} \cdot \left(\varepsilon_c - \frac{\sigma_0}{E_0} \cdot (1 + \varphi) - \varepsilon_{cs} - \varepsilon_T \right) \tag{A.7}$$

Compatibility equation
The hypothesis of Navier and Bernoulli is assumed to be valid in this study thus implying a perfect bond between concrete and steel and a linear strain plane. Hence, the strain of each fiber

can be calculated according to the following formula

$$\varepsilon(y) = \varepsilon_0 + \kappa \cdot \left(y - Y_{ref} \right) \tag{A.8}$$

Equilibrium equation
The equilibrium equations are as stated

$$N = \int_{A_c} \sigma_c \cdot dA_c + \int_{A_s} \sigma_s \cdot dA_s$$
$$M = \int_{A_c} \sigma_c \cdot y \cdot dA_c + \int_{A_s} \sigma_s \cdot y \cdot dA_s \tag{A.9}$$

Instantaneous behavior
To solve the instantaneous behavior of a cross-section the compatibility Eq. (A.8) is introduced into the previously described equilibrium equations, thus transforming into

$$EA_{h,t0} \cdot \varepsilon_{0,t0} + EB_{h,t0} \cdot \kappa_{t0} = N$$
$$EB_{h,t0} \cdot \varepsilon_{0,t0} + EI_{h,t0} \cdot \kappa_{t0} = M \tag{A.10}$$

The solution of these equations is non-linear and requires an iteration process. These equations are the fundamental description of the instantaneous stress field which is the source of the long-term equation's solution.

Long-term behavior
To describe the long-term behavior, the long-term stress variation (A.7) needs to be introduced into the instantaneous equilibrium Eq. (A.9)

$$N = \int_{A_c} \sigma_0 \cdot dA_c + \int_{A_c} \frac{E_c}{1+\chi \cdot \varphi} \cdot \left(\varepsilon_c - \varepsilon_{cs} - \frac{\sigma_0}{E_0} \cdot (1+\varphi) - \varepsilon_T \right) \cdot dA_c + \int_{A_s} E_s \cdot (\varepsilon_s - \varepsilon_T) \cdot dA_s \tag{A.11}$$

$$M = \int_{A_c} \sigma_0 \cdot y \cdot dA_c + \int_{A_c} \frac{E_c}{(1+\chi \cdot \varphi)} \cdot \left(\varepsilon_c - \varepsilon_{cs} - \frac{\sigma_0}{E_0} \cdot (1+\varphi) - \varepsilon_T \right) \cdot y \cdot dA_c + \int_{A_s} E_s \cdot (\varepsilon_s - \varepsilon_T) \cdot y \cdot dA_s$$

Consequently the long-term behavior can be written as

$$EA_{h,t\infty} \cdot \varepsilon_0 + EB_{h,t\infty} \cdot \kappa = N + N_{cs} + N_{cc} + N_T - N_{t0}$$
$$EB_{h,t\infty} \cdot \varepsilon_0 + EI_{h,t\infty} \cdot \kappa = M + M_{cs} + M_{cc} + M_T - M_{t0} \tag{A.12}$$

This equation is a summation of the fictitious internal forces as listed below

$$N_{t0} = EA_{c,t0} \cdot \varepsilon_{0,t0} + EB_{c,t0} \cdot k_{t0} \tag{A.13}$$

$$N_{cc} = \frac{(1+\varphi)}{(1+\chi \cdot \varphi)} \cdot N_{t0} \tag{A.14}$$

$$N_{cs} = EA_c \cdot \varepsilon_{cs} \tag{A.15}$$

$$N_T = EA_h \cdot \varepsilon_T + EB_h \cdot \kappa_T \qquad \text{(A.16)}$$

$$M_{t0} = EB_{c,t0} \cdot \varepsilon_{0,t0} + EI_{c,t0} \cdot \kappa_{t0} \qquad \text{(A.17)}$$

$$M_{cc} = \frac{(1+\varphi)}{(1+\chi \cdot \varphi)} \cdot M_{t0} \qquad \text{(A.18)}$$

$$M_{cs} = EB_c \cdot \varepsilon_{cs} \qquad \text{(A.19)}$$

$$M_T = EB_h \cdot \varepsilon_T \qquad \text{(A.20)}$$